

Supporting information

A Bimetallic Cu-BHQT receptor for selective cysteine detection in extracellular environments via fluorescence quenching-recovery

Sakthivel Vishnu Priya, Thavasilingam Nagendraraj and Jamespandi Annaraj*

1.1. Synthesis of the terephthalohydrazide

Methanolic solution (10 ml) of terephthalic acid (0.5 g) in the presence of con.H₂SO₄ (10:1) was refluxed for 6h. The reaction mixture was cooled to room temperature and evaporated under pressure, provided a dirty white colour solid. The solid formed was extracted with DCM for at least 3 times in order to completely remove the impurities and dried using NaSO₄. The solution was then filtered and evaporated to give milky white solid (1 mmol). Subsequently, it was re-dissolved in methanol followed by slow addition of hydrazine monohydrate (2 mmol) and allowed to reflux for 3 h. The obtained white solid (bis-hydrazine derivative) was filtered, washed with water and dried under vacuum as illustrated in Scheme 1.¹

1.2. Synthesis of the 2-hydroxy quinoline-3-carbaldehyde

2-hydroxy-3-formyl quinoline was synthesised using our earlier reported procedure by Vilsmeier-Haack reaction with phenyl acetamide.² POCl₃ and DMF (3:1) were placed in an ice bath, to this 1eq of phenyl acetamide was slowly added and allowed to stir for 30 mins under nitrogen atmosphere at room temperature. This reaction mixture was allowed to reflux for 6h at 80°C. After completion of the reaction, the mixture was poured in to crushed ice, and the obtained yellow colour precipitated was filtered, dried and recrystallized with ethyl acetate, which was dissolved in acetic acid and water mixture (7:3) and reflux for 2 h. During the reflection, the acetylation followed by hydrolysis was occurred. Reaction mixture was poured to ice and the obtained precipitate was filtered; yield a yellow coloured 2-hydroxy-3-formyl quinolone was obtained.

Supporting information

1.3. Spectral measurement

The ligand of BHQT (1.0×10^{-3} M) is prepared in DMSO stock solution and metal ions and amino acids are made in water (1.0×10^{-2} M). The BHQT was blended with diverse samples in equal portions and the concentration of the chemosensor was 1×10^{-5} mol/L for fluorescence testing, which was executed in a H₂O/MeOH (v/v = 9:1) (pH = 7.24) buffer system.

1.4. Determination of LOD, LOQ and K_a of BHQT detecting Cu²⁺

The detection and quantification limits of BHQT and Cu²⁺ were measured from the titration spectra of BHQT and Cu²⁺. The following equation was used to determine the plot of LOD and LOQ.

$$\text{Slope} = 0.0153 \pm 4.07476\text{E-}4$$

$$R^2 = 0.99366$$

$$S = 0.0153 \quad \delta = \sqrt{\frac{\sum (F_0 - \bar{F}_0)^2}{N - 1}} = 0.09707090$$

$$\text{LOD} = K \times \delta / S = 4.21 \times 10^{-4} \text{ M}$$

$$\text{LOQ} = 10 \times \delta / S = 12.68 \times 10^{-4} \text{ M}$$

The absorbance detection limits and quantification limits of BHQT for Cu²⁺ were measured from the titration spectra of the sensors BHQT - Cu²⁺.

$$\text{Slope} = 17.30358 \pm 0.30571$$

$$R^2 = 0.99318$$

$$S = 17.30358 \quad \delta = \sqrt{\frac{\sum (F_0 - \bar{F}_0)^2}{N - 1}} = 119.843966$$

$$\text{LOD} = K \times \delta / S = 4.57 \times 10^{-4} \text{ M}$$

$$\text{LOQ} = 10 \times \delta / S = 13.8 \times 10^{-4} \text{ M}$$

Where F_0 and \bar{F}_0 are fluorescence intensity and mean of fluorescence intensity of the blank solution of chemosensor **BHQT**, respectively. The δ represents the standard deviation

Supporting information

of the measurement and S represents the slope of the fluorescence intensity versus sample concentration curve.

1.5. Stern Volmer Quenching

To determine the binding constants of Cu^{2+} ion and chemosensor **BHQT**. Fluorescence Absorbance intensity ratio (F_0/F) of **BHQT** versus increasing concentration of $[\text{Cu}^{2+}]$.

$$F_0/F = 1 + K_{SV} [Q]$$

$$K_{SV} = 1/\text{Slope}$$

Where F_0 and F are the emission intensities of the chemosensor before and after the addition of Cu^{2+}

K_{SV} – Stern Volmer constant

Q – Quenching constant

$$K_a = 1.19 \times 10^6 \text{ M}^{-1} \text{ for Fluorescence}$$

$$K_a = 13.7 \times 10^4 \text{ M}^{-1} \text{ for Absorbance}$$

1.6. Determination of LOD, LOQ and K_a of BHQT- Cu^{2+} detecting Cys

The fluorescence detection limits and quantification limits of **BHQT** for Cys were measured from the titration spectra of the sensors **BHQT** and Cys. The following equation was used to determine the plot of LOD and LOQ.

$$\text{Slope} = 0.02768 \pm 7.28185\text{E-}4$$

$$R^2 = 0.99381$$

$$S = 0.02768 \quad \delta = \sqrt{\frac{\sum (F_0 - \bar{F}_0)^2}{N - 1}} = 0.175609685$$

$$\text{LOD} = K \times \delta / S = 4.18 \times 10^{-4} \text{ M}$$

$$\text{LOQ} = 10 \times \delta / S = 12.6 \times 10^{-4} \text{ M}$$

Supporting information

1.7. Determination of Association Constant (K_a):

Association constant was calculated according to the Benesi-Hildebrand equation. K_a was calculated following the equation stated below.

$$1/(A-A_0) = 1/\{K(A_{\max}-A_0) [M^{X^+}]^n\} + 1/[A_{\max}-A_0]$$

Here, A_0 is the absorbance of BHQT in the absence of Cys

A is the absorbance recorded in the presence of added Cys

A_{\max} is absorbance in presence of added $[M^{X^+}]_{\max}$ and

K_a is the association constant, where $[M^{X^+}]$ is [Cys].

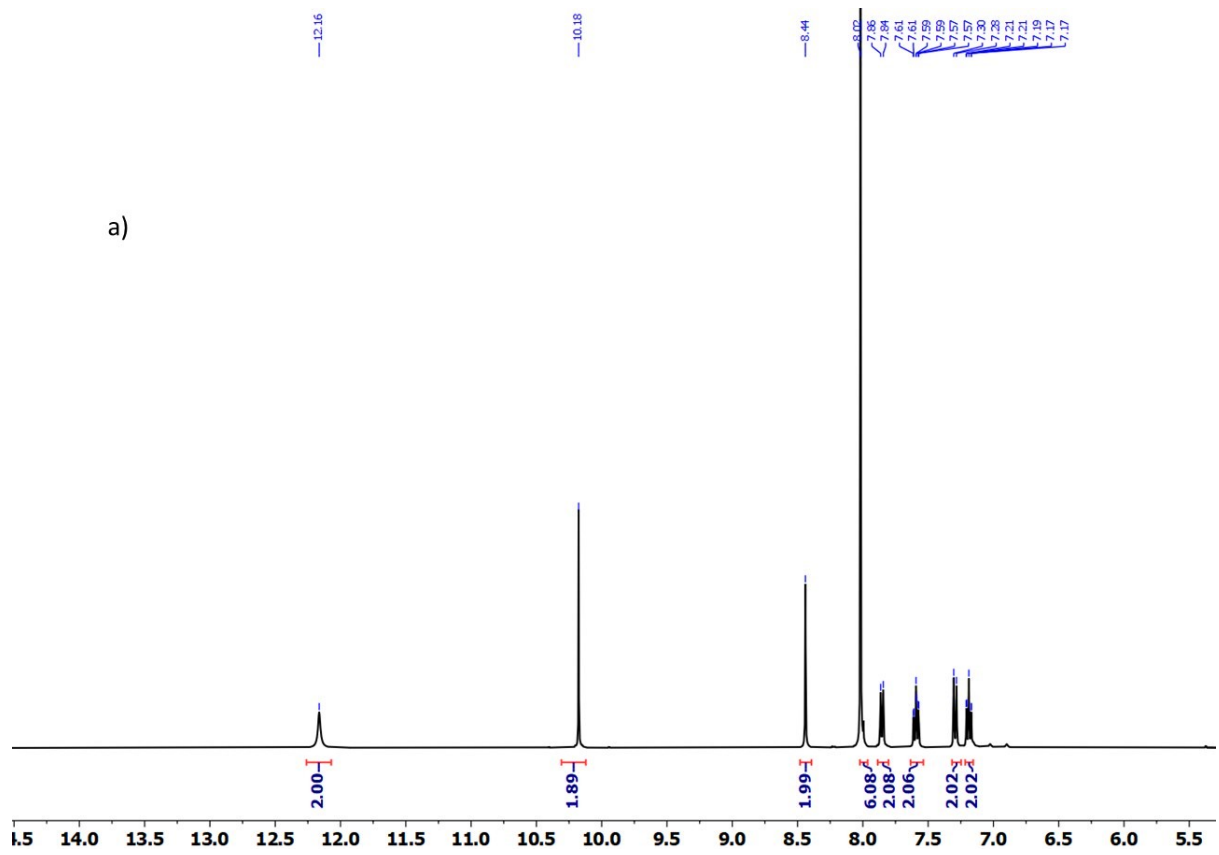
$$\text{Intercept} = 1.004 \pm 0.00764$$

$$\text{Slope} = 0.02418 \pm 4.34125E-4$$

$$R^2 = 0.99551$$

The association constant (K_a) could be determined from the slope of the straight line of the plot of $1/(A-A_0)$ against $1/[Cys]$ and is found to be 8.30×10^{-4} M.

Supporting information



Supporting information

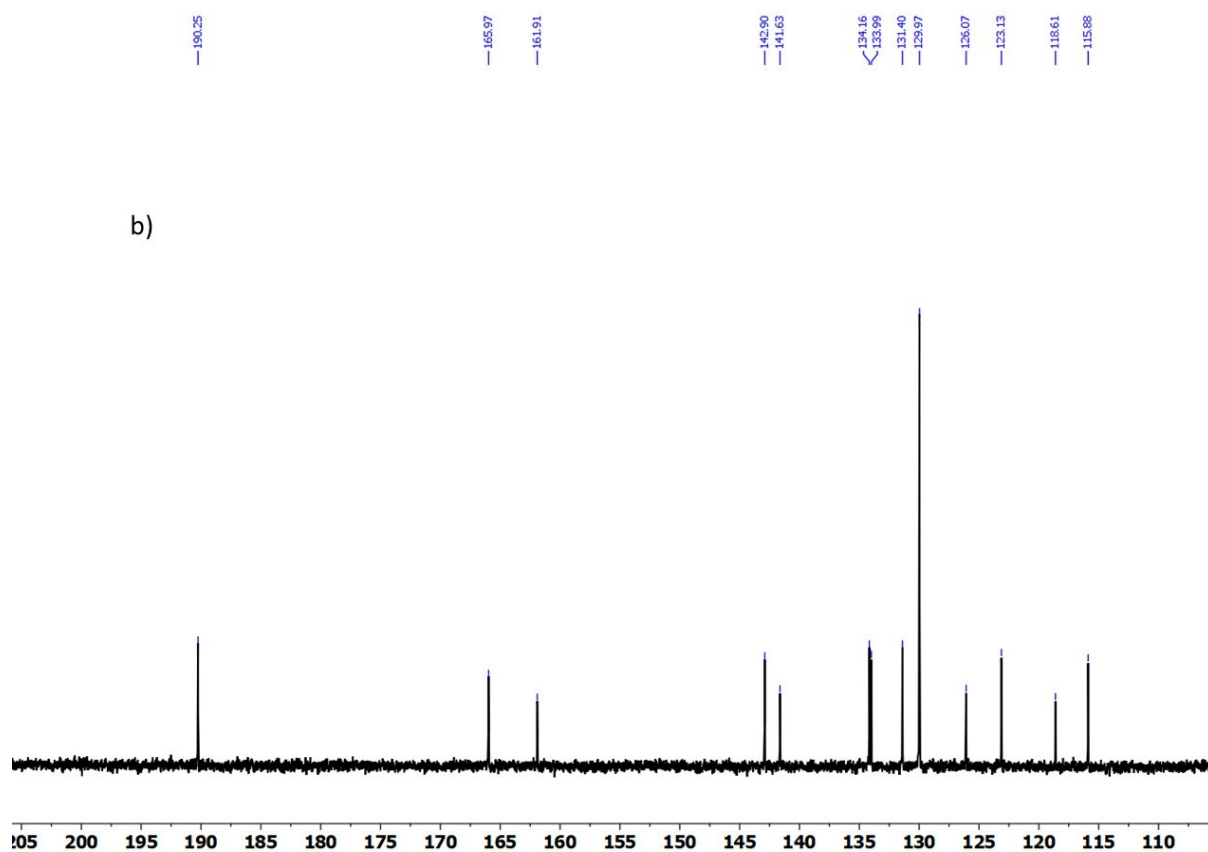


Fig. S1. a) ^1H and b) ^{13}C NMR spectra of BHQT.

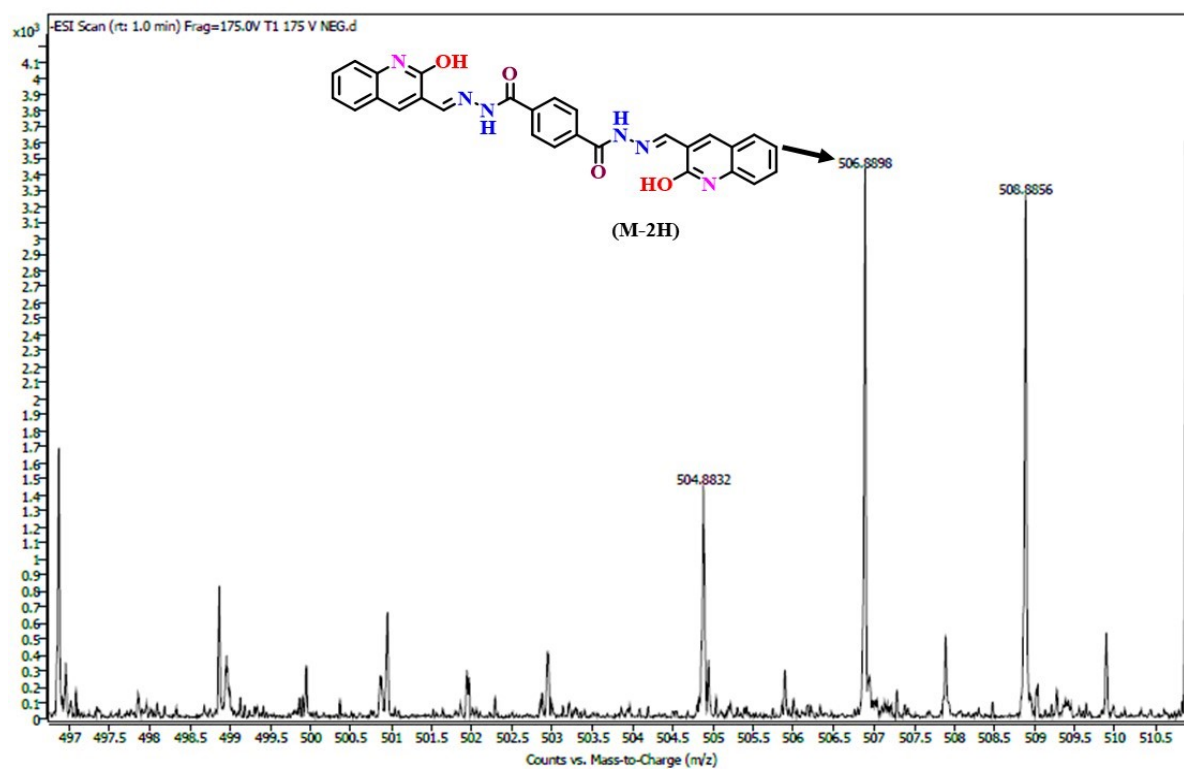


Fig. S2. ESI-MS spectra of BHQT.

Supporting information

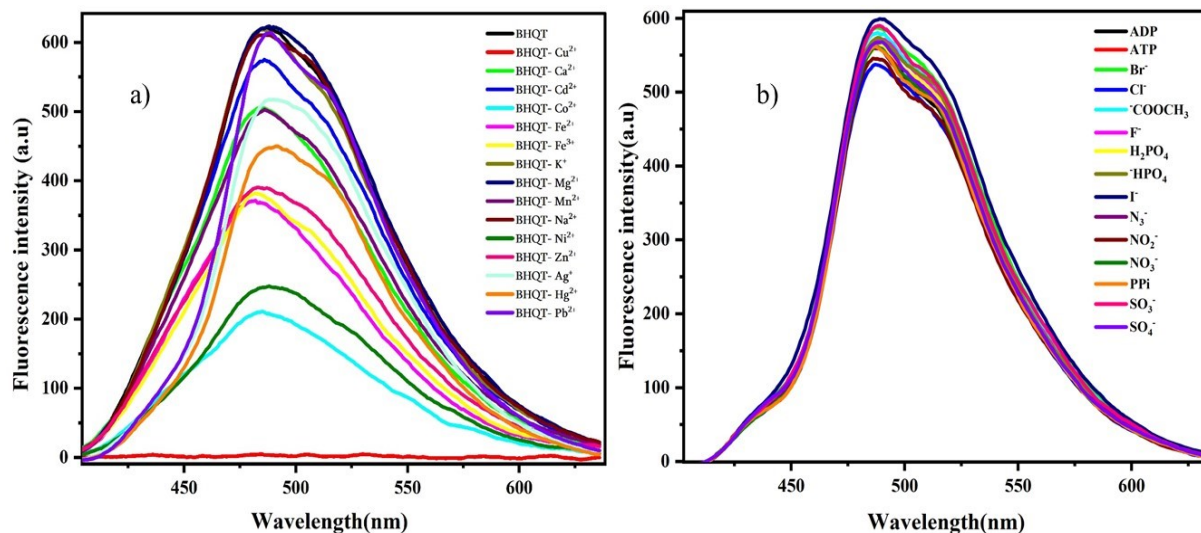


Fig. S3. The fluorescence spectra of BHQT with 10 equiv. of various a) cations, and b) anions in water: MeOH (9:1) solution.

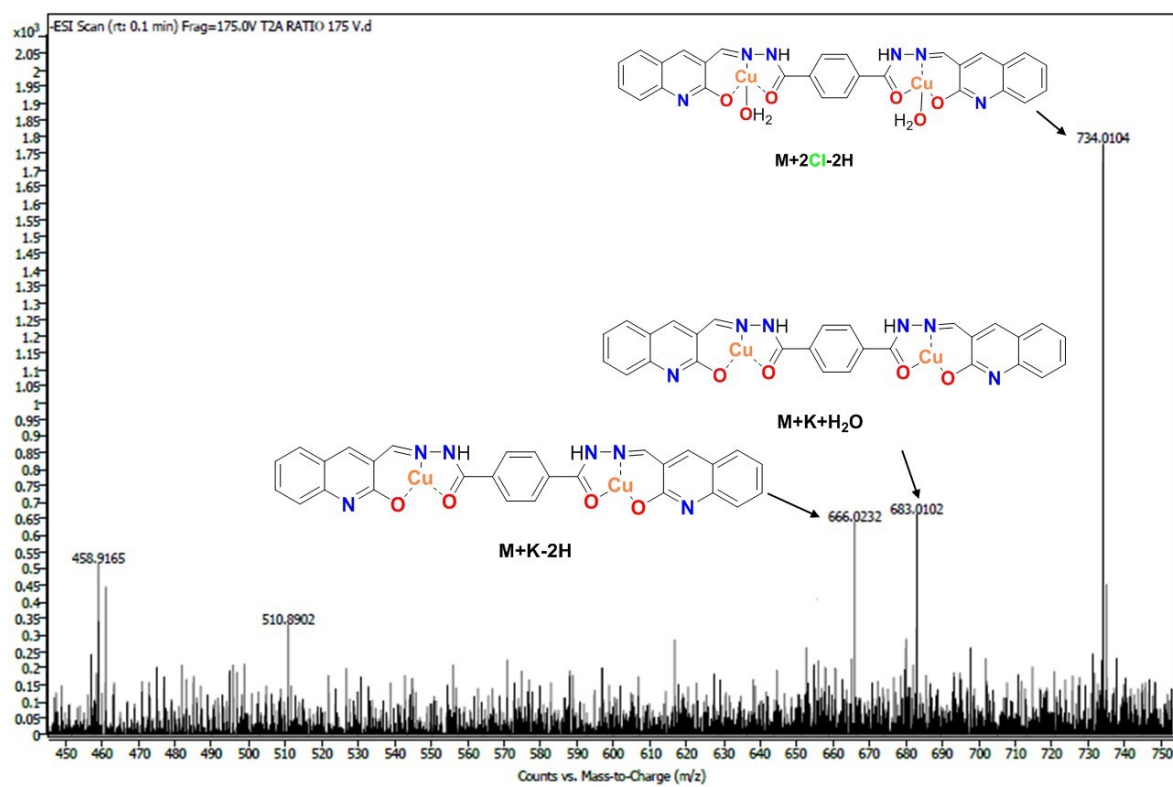


Fig. S4. ESI-MS spectra of mixture BHQT and Cu^{2+} (1:2).

Supporting information

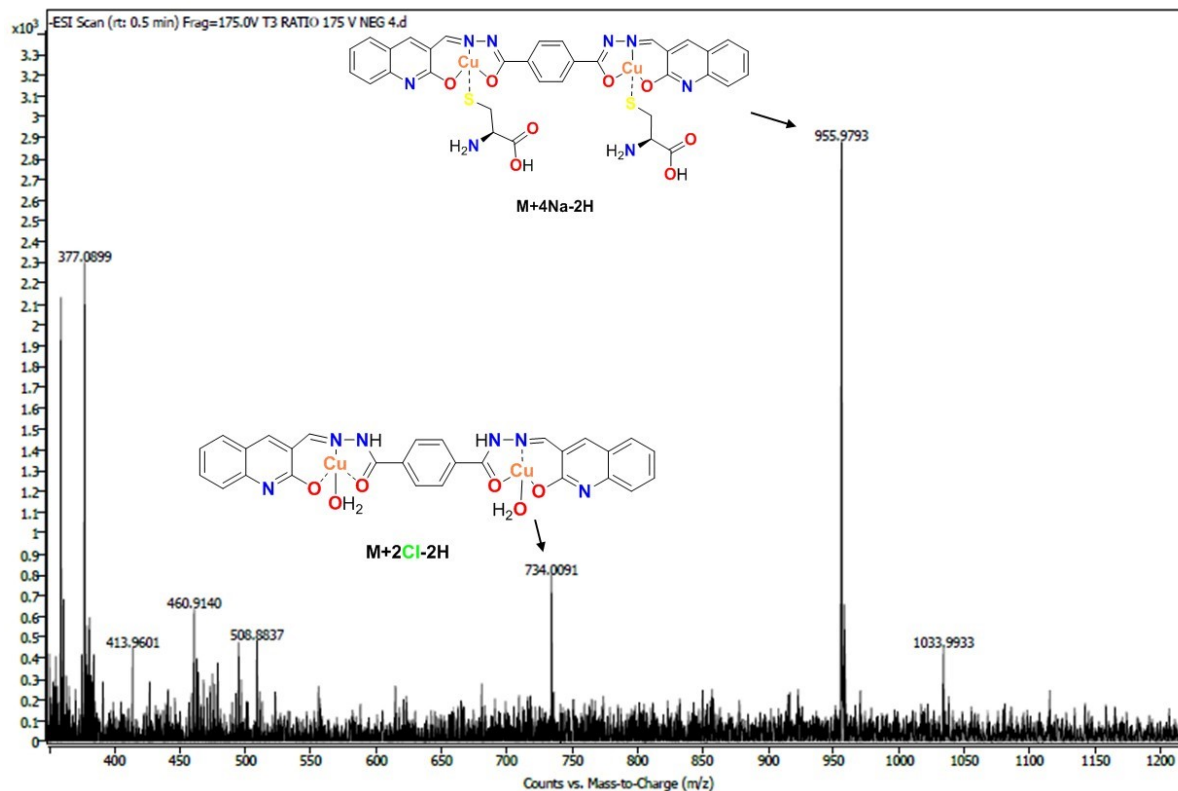


Fig. S5. ESI-MS spectra of reaction between BHQT-Cu and 2 equiv. of Cys.

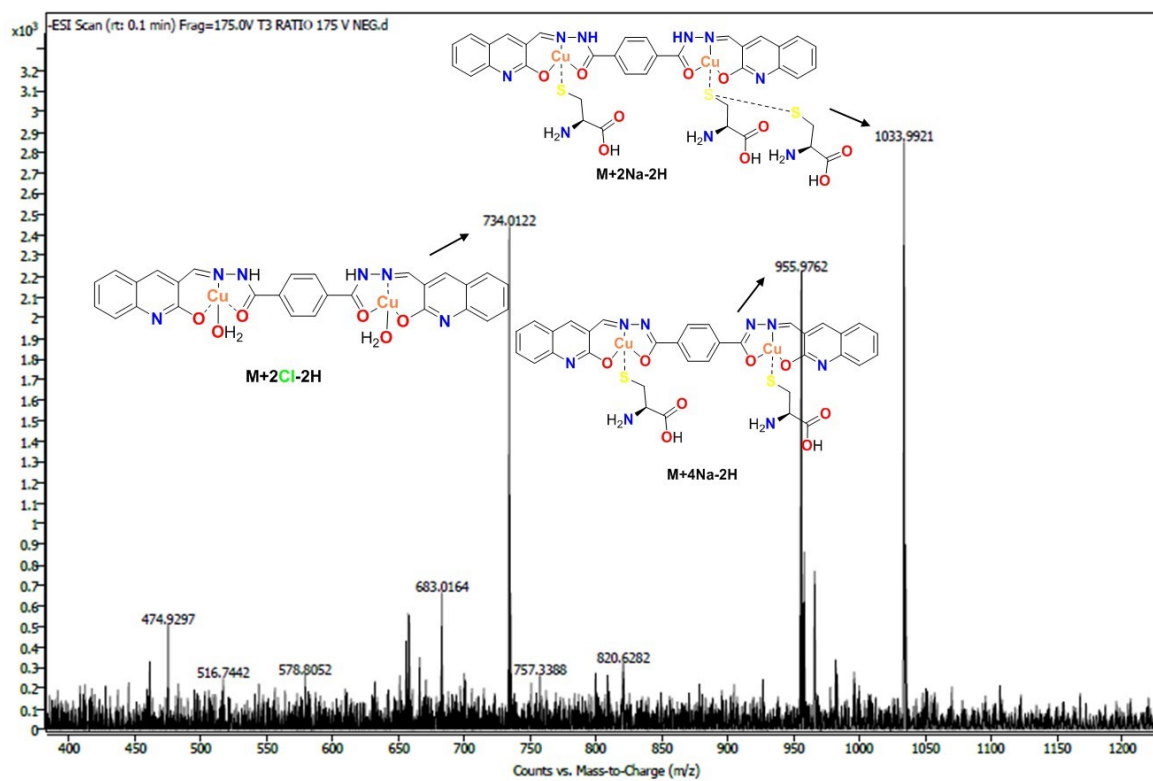


Fig. S6. ESI-MS spectra of the interaction of BHQT-Cu with 4 equiv. of Cys.

Supporting information

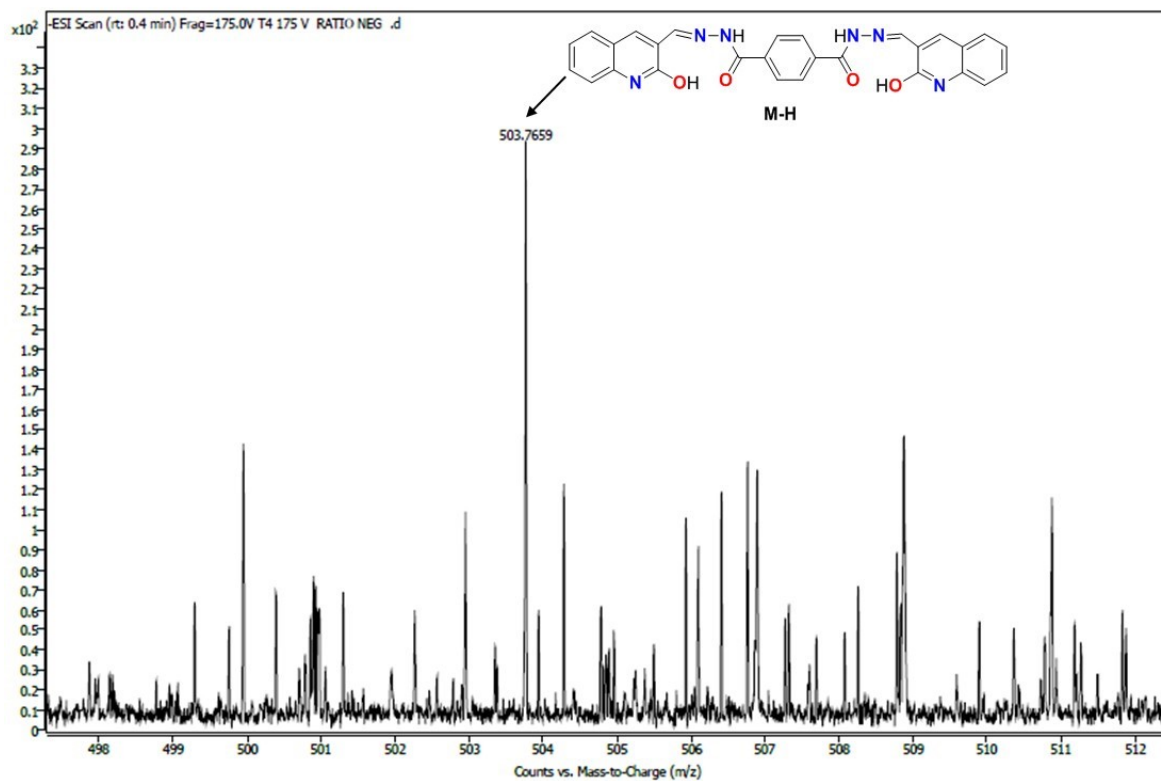
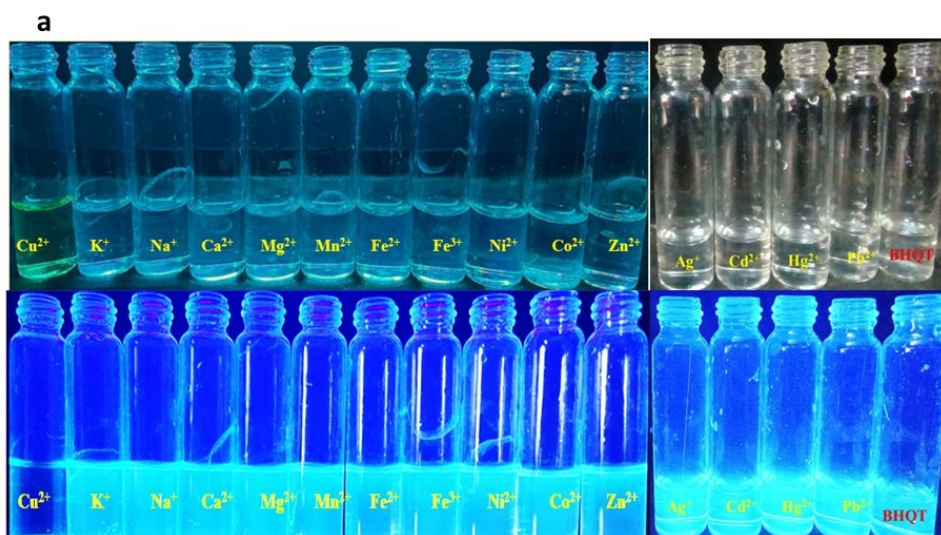


Fig. S7. ESI-MS spectra of interaction of BHQT-Cu with 10 equiv. of Cys.



Supporting information

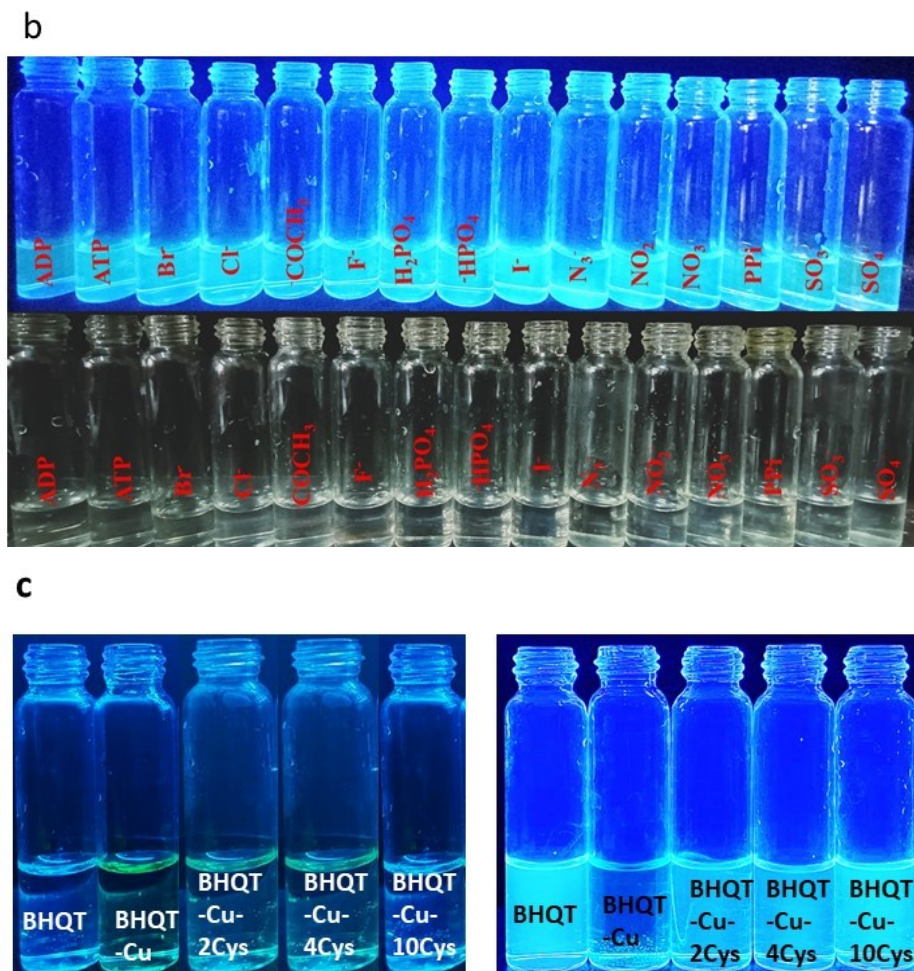
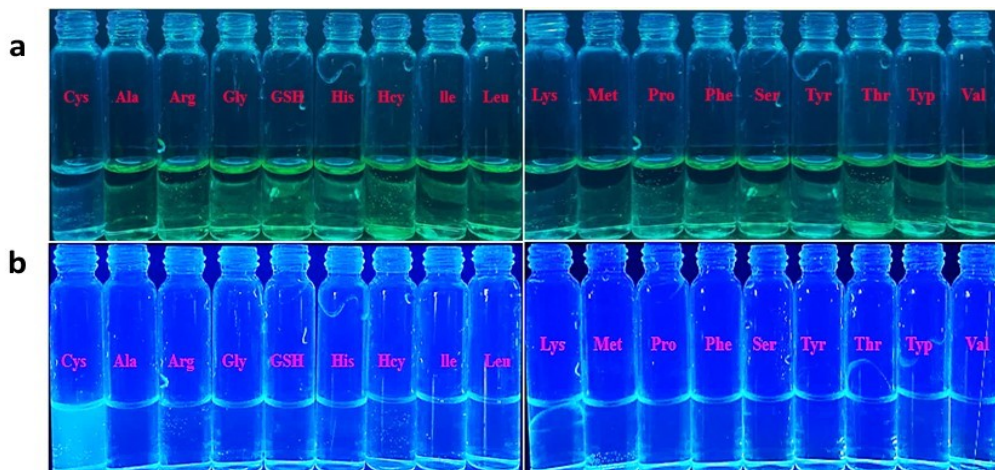


Fig.S8 a) Visible light and Fluorescence colour change of the chemosensor BHQT (1.0×10^{-5} M) upon addition of various metal cations (Ag^+ , Cu^{2+} , K^+ and Na^+ , Ca^{2+} , Cd^{2+} , Hg^{2+} , Mg^{2+} , Mn^{2+} , Fe^{2+} , Fe^{3+} , Ni^{2+} , Co^{2+} , Pb^{2+} , Zn^{2+} and BHQT) and b) anions (ADP , ATP , Br^- , Cl^- , COOCH_3 , F^- , H_2PO_4^- , HPO_4^- , I^- , N_3^- , NO_2^- , NO_3^- , PPI , SO_3^- , SO_4^-), c) BHQT showing quenching with Cu^{2+} and recovery Cysteine (2–10 equiv.) under 365 nm UV lamp.



Supporting information

Fig.S9 (a) The color of the chemosensor BHQT- Cu^{2+} (1.0×10^{-5} M) solution with different amino acids added under natural light. (b) Fluorescence color change of the chemosensor BHQT (1.0×10^{-5} M) upon addition of various amino acids (Cys, Ala, Arg, Gly, GSH, His, Hcy, Ile, Leu, Lys, Met, Pro, Phe, Ser, Tyr, Thr, Typ and Val) under excitation at 380 nm.

Table-S1. Fluorescence lifetime Parameters of BHQT towards Cu^{2+} and Cys.

System	λ_{ex} nm	λ_{em} nm	$\tau_1(\text{ns})$ (Rel%)	$\tau_2(\text{ns})$ (Rel%)	$\tau_3(\text{ns})$ (Rel%)	τ average(ns))	χ^2
BHQT	380	488	1.94824	4.14293	0.549438	2.2ns	1.029512
BHQT- Cu^{2+}	380	488	1.24061	2.79025	0.343234	1.4ns	1.119726
BHQT- Cu^{2+} + 2 equiv. Cys	380	488	1.1627	3.06908	0.300993	1.5ns	1.001995
BHQT- Cu^{2+} + 4 equiv. Cys	380	488	1.136	3.01459	0.138198	1.3ns	1.0495
Probe- Cu^{2+} + 10 equiv. Cys	380	488	1.66161	3.86507	0.400953	2.17ns	1.0901

1.8. Extracting food sample analysis

The sample testing system for extracting food samples (apple, radish, garlic, mint, and onion) consisted of 1.98 mL of a H_2O : MeOH (9:1) mixture with HEPES buffer (10 mM, pH 7.4), 0.04 mL of the stock solution of BHQT- Cu^{2+} , and 0.02 mL of the respective food sample. Various concentrations of Cys ranging from 0 to 40 μM (2×10^{-5} M) were added to the solution. The

Supporting information

prepared mixture was then transferred into a quartz cell for detection. Absorbance spectra were recorded in the range of 300 to 450 nm.

1.8.1. Preparation of food sample extracts

For the precise determination of cysteine, a selection of protein-rich processed or canned food samples, including apple, radish, garlic, mint, and onion, were chosen from our food regime. Five grams of each sample were prepared for the experiment. Initially, all samples were thoroughly cleared, washed, and finely minced, followed by drying at 65°C for 4 to 5 hours. Once dried, the samples were separately ground in pestle and mortars, then transferred to round-bottom flasks. To each flask, 15 mL of 6 M HCl was added, and the mixture was subjected to hydrolysis for 24 hours at 110°C. After hydrolysis, the reaction mixture was cooled to room temperature and neutralized by adding solid Na₂CO₃. The resulting solution was then diluted to a final volume of 100 mL using 10 mM HEPES-buffered solution (pH 7.0) and filtered. The obtained filtrate was directly utilized for the quantification of cysteine, as the employed probe is highly selective for cysteine over all other amino acids present in the protein samples under investigation.⁴⁻⁸

[Concentration of L- Cysteine spiked: 4 μM -40 μM].

Sample	Amount of L-Cysteine determined in HEPES	Absorbance	Amount of L-Cysteine spiked in food sample	Absorbance	Recovery and RSD (%)
Apple	4	0.57	4	0.59	103 ± 1.09 %
	8	0.54	8	0.57	105 ± 1.0%
	12	0.53	12	0.55	103 ± 1.79%
	16	0.51	16	0.52	101 ± 0.97%
	20	0.50	20	0.50	100 ± 1.96%
	24	0.49	24	0.49	100 ± 2.0%
	28	0.48	28	0.48	100 ± 1.25%
	32	0.47	32	0.46	97 ± 0.99%
	36	0.46	36	0.45	97± 0.711%
	40	0.45	40	0.44	97 ± 2.27%
Garlic	4	0.57	4	0.54	94 ± 1.08%
	8	0.54	8	0.54	100±1.08%
	12	0.53	12	0.53	100±1.03%
	16	0.51	16	0.51	100±0.22%
	20	0.50	20	0.50	100± 1.16%

Supporting information

	24	0.49	24	0.49	100±1.19%
	28	0.48	28	0.49	102±1.19%
	32	0.47	32	0.47	100 ± 1.22%
	36	0.46	36	0.46	100 ±1.08%
	40	0.45	40	0.41	91 ±1.33%
	4	0.51	4	0.56	109 ±1`09%
	8	0.49	8	0.53	108± 0.987%
	12	0.47	12	0.51	108±0.48%
	16	0.46	16	0.48	104 ±1.35%
Mint	20	0.44	20	0.46	105± 1.33%
	24	0.43	24	0.44	102 ±1.2%
	28	0.42	28	0.43	102 ±0.23%
	32	0.40	32	0.40	100±1.36%
	36	0.39	36	0.39	100 ±1.4%
	40	0.39	40	0.38	97 ± 1.38%
	4	0.51	4	0.48	94±2.13%
	8	0.49	8	0.46	89 ±1.26%
	12	0.47	12	0.43	86 ±1.27%
	16	0.46	16	0.41	86 ±2.38%
Onion	20	0.44	20	0.38	83 ±1.7%
	24	0.43	24	0.37	87 ±1.26%
	28	0.42	28	0.35	84 ±1.88%
	32	0.40	32	0.35	87±1.92%
	36	0.39	36	0.33	84 ±1.65%
	40	0.39	40	0.31	80 ± 1.69%
	4	0.51	4	0.48	94±1.28%
	8	0.49	8	0.47	95 ±0.21%
	12	0.47	12	0.45	95±0.22%
	16	0.46	16	0.42	91 ±1.3%
Radish	20	0.44	20	0.40	90 ±0.38%
	24	0.43	24	0.39	90±0.39%
	28	0.42	28	0.37	88±1.57%
	32	0.40	32	0.35	87±1.67%
	36	0.39	36	0.35	89±0.16%
	40	0.39	40	0.34	87±1.8%

Table S2. Determination of Cys concentration in Food.

1.8.2. Determination of Recovery percentage

Calculation

Apple

At lower concentration of Cysteine (4µM)

Recovery (%) = [Absorbance of Cysteine added /

Supporting information

$$\begin{aligned} & \text{Absorbance of Cysteine determined] X 100.} \\ & = 0.59/0.57 \times 100 \\ & = 103\% \end{aligned}$$

Garlic

At lower concentration of Cysteine (4 μ M)

Recovery (%) = [Absorbance of Cysteine added /

$$\begin{aligned} & \text{Absorbance of Cysteine determined] X 100.} \\ & = 0.54/0.59 \times 100 \\ & = 94\% \end{aligned}$$

Mint

At lower concentration of Cysteine (4 μ M)

Recovery (%) = [Absorbance of Cysteine added /

$$\begin{aligned} & \text{Absorbance of Cysteine determined] X 100.} \\ & = 0.56/0.51 \times 100 \\ & = 109\% \end{aligned}$$

Onion

At lower concentration of Cysteine (4 μ M)

Recovery (%) = [Absorbance of Cysteine added /

$$\begin{aligned} & \text{Absorbance of Cysteine determined] X 100.} \\ & = 0.48/0.51 \times 100 \\ & = 94\% \end{aligned}$$

Radish

At lower concentration of Cysteine (4 μ M)

Recovery (%) = [Absorbance of Cysteine added /

$$\begin{aligned} & \text{Absorbance of Cysteine determined] X 100.} \\ & = 0.48/0.51 \times 100 \\ & = 94\% \end{aligned}$$

1.8.3. Determination of Relative Standard Deviation (RSD)

$$\text{RSD} = \text{S.D} / \bar{x}$$

Where SD is the standard deviation and \bar{x} mean value of the sample data set.

Supporting information

Apple

At lower concentration of Cysteine (4 μ M)

S. D = 0.0064

\bar{x} = 0.58

No of trials (N) =3

RSD = 0.0064/0.58= 1.09%

At medium concentration of Cysteine (20 μ M)

S. D = 0.01

\bar{x} = 0.51

No of trials (N) =3

RSD = 0.01/0.51= 1.96 %

At higher concentration of Cysteine (40 μ M)

S. D = 0.01

\bar{x} = 0.44

No of trials (N) =3

RSD = 0.01/0.44

= 2.27 %

Garlic

At lower concentration of Cysteine (4 μ M)

S. D = 0.0057

\bar{x} = 0.533

No of trials (N) =3

RSD = 0.0057/0.533= 1.08%

At medium concentration of Cysteine (20 μ M)

S. D = 0.0057

\bar{x} = 0.4966

No of trials (N) =3

RSD = 0.0057/0.4966= 1.16%

At higher concentration of Cysteine (40 μ M)

S. D = 0.0055

\bar{x} = 0.413

Supporting information

No of trials (N) =3
RSD = 0.0055/0.413
= 1.33 %

Mint

At lower concentration of Cysteine (4 μ M)

S. D = 0.00608
 \bar{x} = 0.557
No of trials (N) =3
RSD = 0.00608/0.557= 1.09%

At medium concentration of Cysteine (20 μ M)

S. D = 0.006083
 \bar{x} = 0.457
No of trials (N) =3
RSD = 0.006083/0.457 = 1.33%

At higher concentration of Cysteine (40 μ M)

S. D = 0.005292
 \bar{x} = 0.384
No of trials (N) =3
RSD = 0.00529/0.384
= 1.38 %

Onion

At lower concentration of Cysteine (4 μ M)

S. D = 0.01
 \bar{x} = 0.47
No of trials (N) =3
RSD = 0.01/0.47= 2.13 %

At medium concentration of Cysteine (20 μ M)

S. D = 0.0064
 \bar{x} = 0.377
No of trials (N) =3
RSD = 0.0064/0.377= 1.7 %

Supporting information

At higher concentration of Cysteine (40 μ M)

S. D = 0.0052
 \bar{x} = 0.314
No of trials (N) =3
RSD = 0.0052/0.314
= 1.69 %

Radish

At lower concentration of Cysteine (4 μ M)

S. D = 0.006
 \bar{x} = 0.477
No of trials (N) =3
RSD = 0.006/0.477= 1.28 %

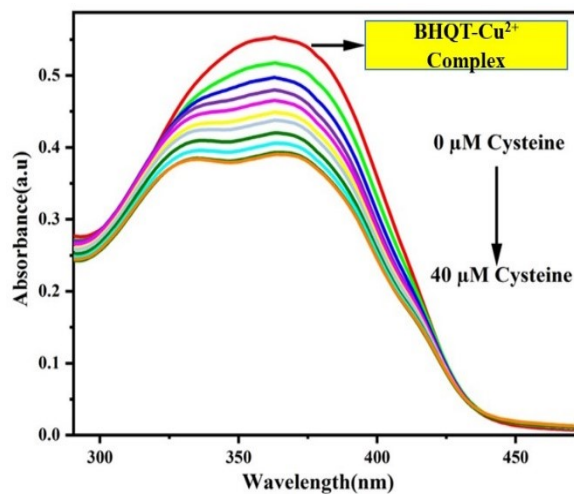
At medium concentration of Cysteine (20 μ M)

S. D = 0.00152
 \bar{x} = 0.4013
No of trials (N) =3
RSD = 0.00152/0.4013= 0.38 %

At higher concentration of Cysteine (40 μ M)

S. D = 0.006
 \bar{x} = 0.337
No of trials (N) =3
RSD = 0.006/0.337
= 1.8 %

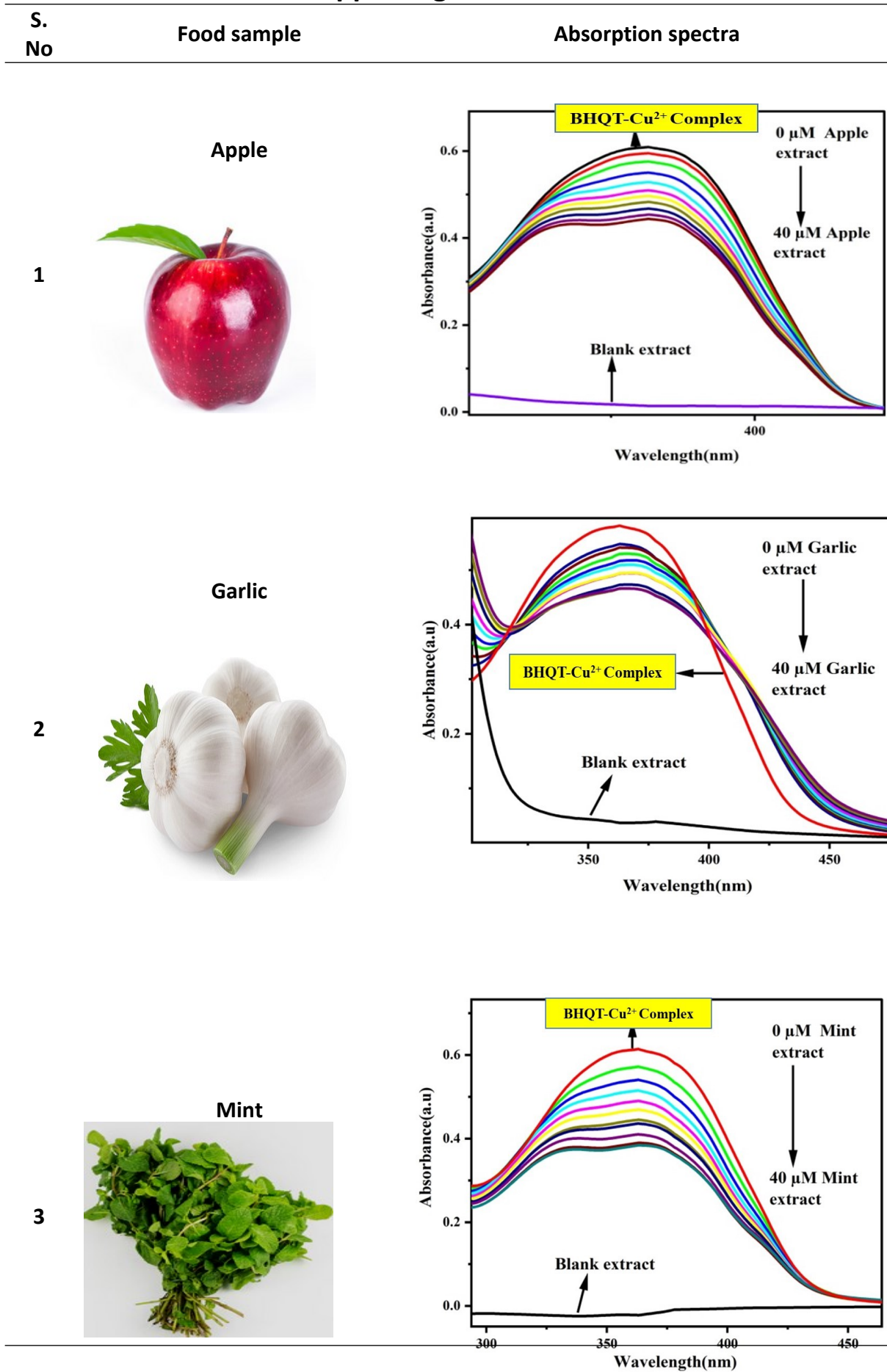
Absorbance spectra of L- Cysteine Hydrochloride Commercial Material.



Supporting information

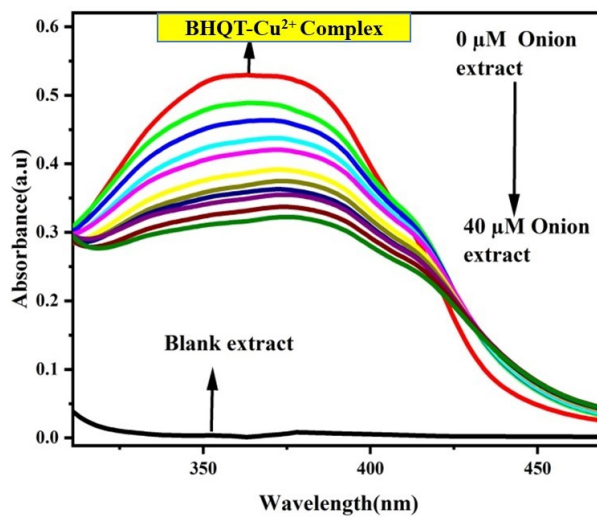
Fig.S10. Sensitivity of L-Cysteine (0 μM - 40 μM) towards BHQT-Cu²⁺ in H₂O – MeOH (9:1) HEPES buffer medium (pH – 7.24).

Supporting information



Supporting information

4



5

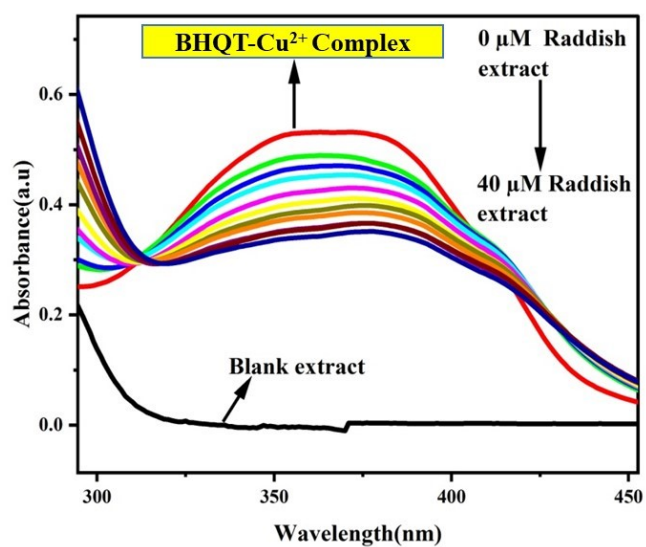
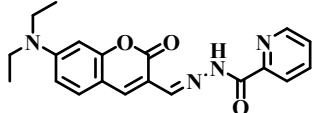
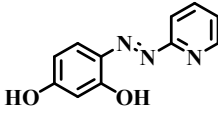
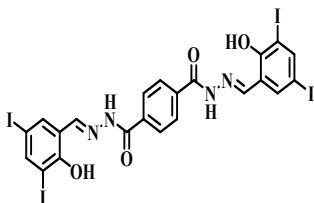
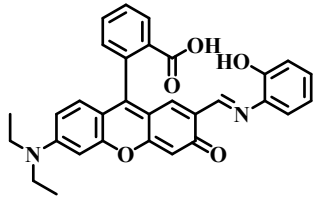
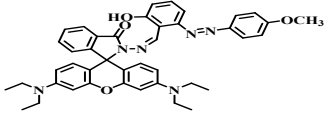


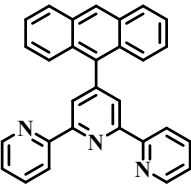
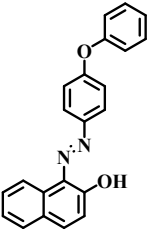
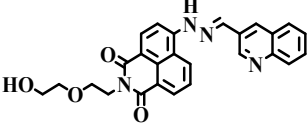
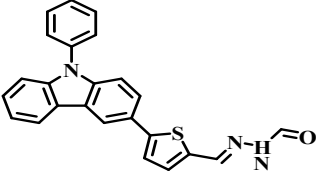
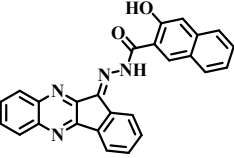
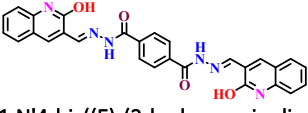
Table.S3. Absorption spectrum for the detection of L- Cysteine in food samples.

Supporting information

Comparison table. S4

S. no	Probe	Solvent	Detection of analytes	λ_{ex} nm	λ_{em} nm	Binding constant		LOD		Ref.
						Probe + Cu ²⁺	Probe + Cu ²⁺ + Cys	Probe + Cu ²⁺	Probe + Cu ²⁺ + Cys	
1.	 <p>N'-((7-(diethylamino)-2-oxo-2H-chromen-3-yl)methylene)picolinohydrazide</p>	MeOH: H ₂ O (1:1, v/v) tris buffer	Cys	390	51 5	1.45 × 10 ⁵ M ⁻¹	6.18 ×10 ⁸ M ⁻²	9.3 × 10 ⁻⁷ M	5.83 × 10 ⁻⁶ M	9
2.	 <p>4-(2-pyridylazo) resorcinol</p>		Cys	412 nm	-	2 × 10 ⁴ M ⁻¹	1.3 × 10 ³ M ⁻¹	4.8 × 10 ⁻⁷ M	7.82 × 10 ⁻⁶ M	10
3.	 <p>N'1,N'4-bis((E)-2-hydroxy-3,5-diiodobenzylidene)terephthalohydrazide</p>	CH ₃ CN : H ₂ O (7:3, v/v) HEPES buffer at 7.2	Cys	430	55 0	4.93 × 10 ¹⁰ M ⁻²	0.95 × 10 ⁴ M ⁻¹	7.3 × 10 ⁻⁶ M	36 × 10 ⁻⁶ M	11
4.	 <p>(E)-2-(6-(diethylamino)-2-((2-hydroxyphenylimino)methyl)-3-oxo-3H-xanthen-9-yl)benzoic acid</p>	DMSO: H ₂ O (8:2) solution	Cys	335	54 9	1.7 × 10 ⁻² M	1.6 × 10 ² M ⁻¹	2 × 10 ⁻⁷ M	55 × 10 ⁻⁹ M	12
5.	 <p>3',6'-bis(diethylamino)-2-(((Z)-2-hydroxy-6((4-methoxyphenyl)diazonyl)benzylidene)amino)spiro[isindoline-1,9'-xanthen]-3-one</p>	MeOH: H ₂ O (3:7, v/v) solution	Cys	535	58 8	-	-	-	1.2 × 10 ⁻⁶ M	13

Supporting information

6.	 <p>4'-(anthracen-9-yl)-2,2':6',2''-terpyridine</p>	MeCN: H ₂ O (7:3) at pH 7.34	Cys	366	43 1			$7.7 \times 10^4 \text{ M}^{-1}$	$1.9 \times 10^{-8} \text{ M}$	14
7.	 <p>(E)-1-((4-phenoxyphenyl) diazenyl)naphthalen-2-ol</p>	DMF/H ₂ O (1:9, v/v)	Cys	470	575	$7.72 \times 10^7 \text{ M}^{-1}$	$1.75 \times 10^5 \text{ M}^{-1}$	$11.3 \times 10^{-7} \text{ M}$	$84 \times 10^{-9} \text{ M}$	15
8.	 <p>(E)-2-(2-(2-hydroxyethoxy)ethyl)-6-(2-(quinolin-3-ylmethylene)hydrazineyl)-1H-benzo[de]isoquinoline-1,3(2H)-dione</p>	MeCN/ H ₂ O (3:7, v/v)	Cys	471	549	$4.41 \times 10^4 \text{ M}^{-1}$	$5.2 \times 10^4 \text{ M}^{-1}$	$3.4 \times 10^8 \text{ M}^{-1}$	$4.2 \times 10^8 \text{ M}^{-1}$	16
9.	 <p>2-((5-(9-phenyl-9H-carbazol-3-yl) thiophene-2-yl)-L3-methylene)-1L2-diazane-1-formaldehyde</p>	DMSO- H ₂ O (6:4, v/v)	Cys	372	490	$0.514 \times 10^6 \text{ M}^{-1}$	$1.61 \times 10^{14} \text{ M}^{-2}$	$0.14 \times 10^6 \text{ M}^{-1}$	$52 \times 10^{-9} \text{ M}$	17
10.	 <p>(E)-3-hydroxy-N'-(11H-indeno[1,2-b]quinoxalin-11-ylidene)-2-naphthohydrazide</p>	MeOH- HEPES (1:1, v/v, pH = 7. 4)	Cys	338	393	$1.13 \times 10^4 \text{ M}^{-1}$	$1.03 \times 10^9 \text{ M}^{-2}$	$2.3 \times 10^6 \text{ M}^{-1}$	$60 \times 10^9 \text{ M}^{-1}$	18
11.	 <p>N'1,N'4-bis((E)-(2-hydroxyquinolin-3-yl)methylene)terephthalohydrazide</p>	MeOH/ H ₂ O (1:9, v/v)	Cys	380	488	$1.19 \times 10^{-6} \text{ M}$	$8.3 \times 10^{-4} \text{ M}$	$4.5 \times 10^{-4} \text{ M}$	$4.18 \times 10^{-4} \text{ M}$	Present work

Supporting information

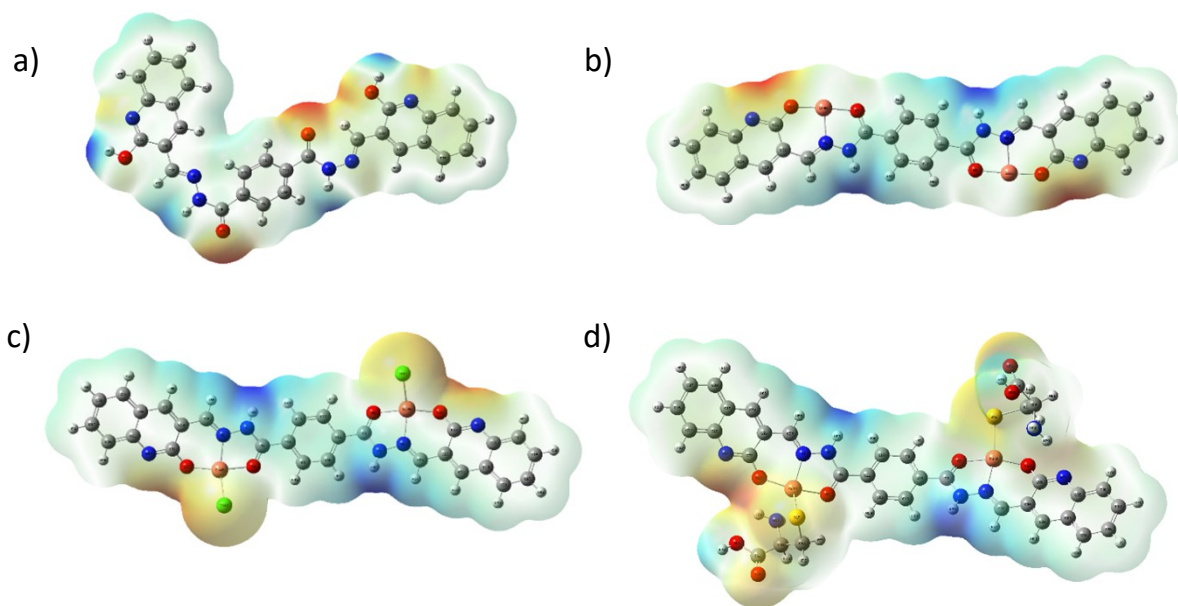


Fig. S11. ESP Mapping corresponding to the complexes a. BHQT b. BHQT- Cu⁺ c. BHQT- Cu²⁺

d. BHQT- Cu²⁺- Cys

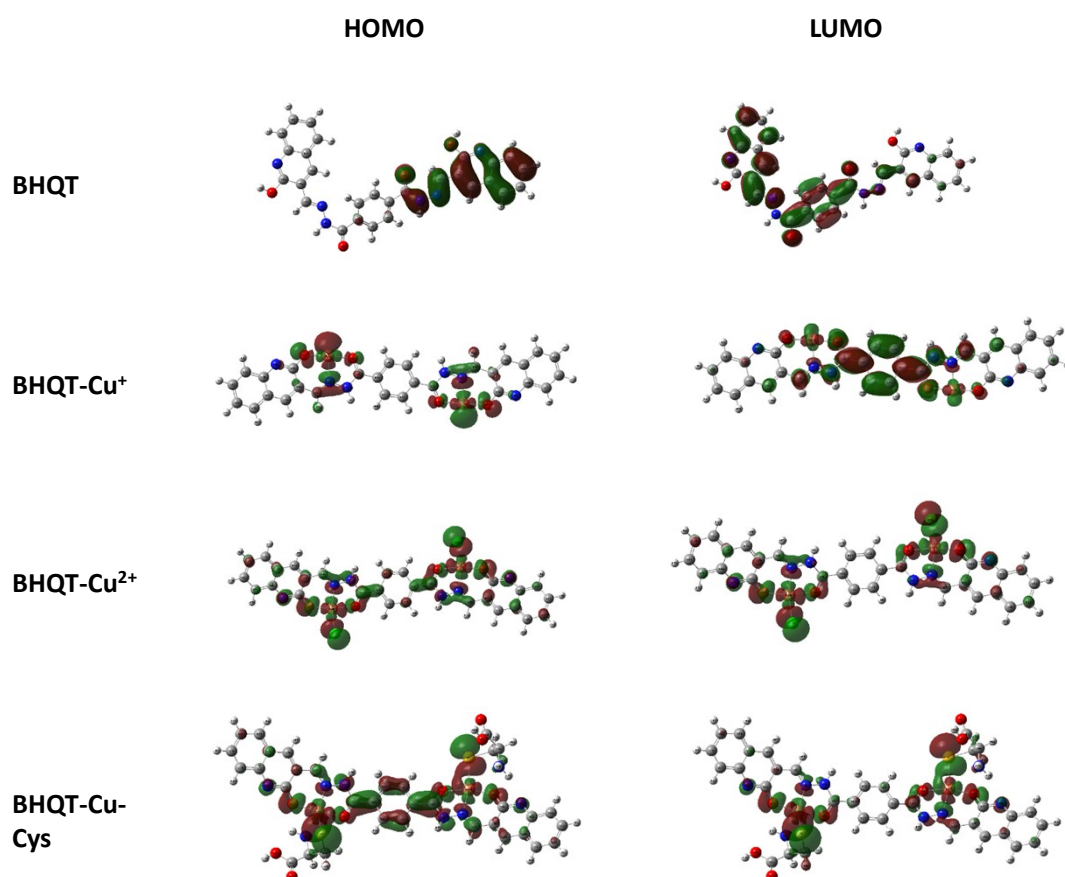


Fig. S12. Electron density distributions of the Frontier Molecular Orbitals (FMOs) showing HOMO and LUMO corresponding to a. BHQT b. BHQT- Cu⁺ c. BHQT- Cu²⁺, d. BHQT- Cu- Cys.

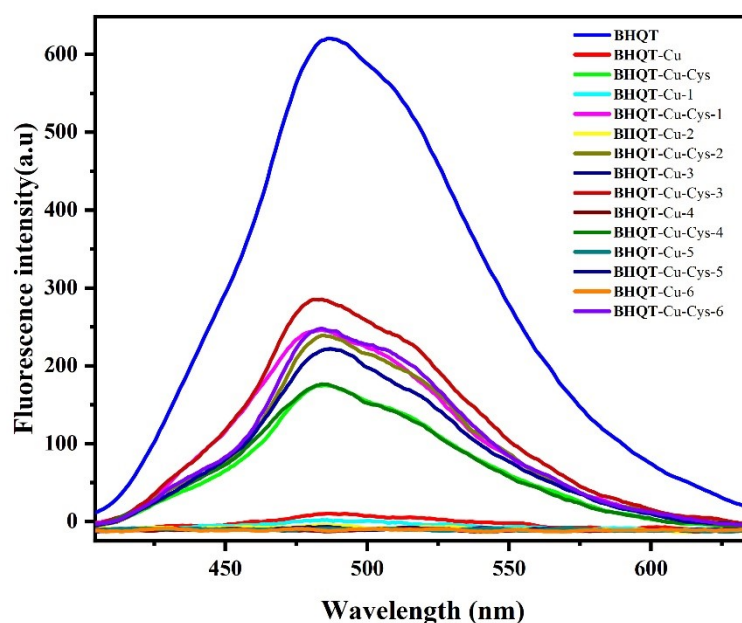
Supporting information

The absolute photoluminescence quantum yield (QY) of the sample was measured using an integrating sphere setup (HORIBA system). The sample was excited over the wavelength range of 360.14 nm to 399.98 nm, and the emission was collected from 400.17 nm to 680.00 nm. The quantum yield was founded to be 6.50%, 0.74 % 1.11 %, 2.75% and 6.20% indicating moderate emission efficiency. This implies that out of all absorbed photons, approximately 6.5% were re-emitted as fluorescence, while the remainder were lost via non-radiative processes. These measurements were corrected against a blank and include an absolute error of ± 0.071 and a relative error of ± 0.01091 .

S.NO	Sample name	$\lambda_{ex}/\lambda_{em}$	Quantum yield
1.	BHQT	380/488	6.50 %
2.	BHQT-Cu ²⁺	380/488	0.74 %
3.	BHQT-Cu ²⁺ - 2 equiv. Cys	380/488	1.11 %
4.	BHQT-Cu ²⁺ - 4 equiv. Cys	380/488	2.75
5.	BHQT-Cu ²⁺ - 10 equiv. Cys	380/488	6.20%

Table.S5. Absolute fluorescence quantum yields of the BHQT, BHQT-Cu²⁺, BHQT-Cu²⁺- 2Cys, BHQT-Cu²⁺- 4Cys, BHQT-Cu²⁺- 10 Cys, in H₂O: MeOH (9:1) (excitation/emission slit width:2/2).

Supporting information



Reversibility Fluorescence Spectra

Fig.S13 Reversibility study of BHQT fluorescence response toward alternating addition of Cu^{2+} and Cys over multiple cycles in fluorescence intensity.

References

1. Senthil Murugan, E. Abel Noelson and J. Annaraj, *Inorg. Chim. Acta*, **2016**, 450.
2. A. Senthil Murugan, N. Vidhyalakshmi, U. Ramesh and J. Annaraj, *J. Mater. Chem. B*, **2017**, 5, 3195–3200.
3. K. Aich, S. Goswami, S. Das and C. D. Mukhopadhyay, *RSC Adv.*, **2015**, 5, 39.
4. Y. Zhiqiang, X. Kang, J. Li, L. Li, X. Ye, X. Liu, K. Chen *et al.*, *Food Chem.*, **2024**, 140064.
5. L. Kai, H. Gu, Y. Sun, X. Chao, S. Yang and B. Zhu, *Food Chem.*, **2021**, 356, 129658.
6. G. Shuai, A. Qin, Y. Zhang, M. Li, X. Chen, Y. Liang, X. Xu, Z. Wang and S. Wang, *Food Chem.*, **2023**, 400, 134108.
7. D. Sujoy, A. Ghosh, S. Kundu, S. Saha, H. S. Sarkar and P. Sahoo, *Anal. Bioanal. Chem.*, **2019**, 411, 6203–6212.
8. X. Yang, J. Wang, Z. Zhang, B. Zhang, X. Du, J. Zhang and J. Wang, *Food Chem.*, **2023**, 416, 135730.
9. Y. Xie, L. Yan and J. Li, *Appl. Spectrosc.*, **2019**, 73, 794–800.
10. H. Tavallali, G. Deilamy-Rad, M. A. Karimi and E. Rahimy, *Anal. Biochem.*, **2019**, 583, 113376.
11. A. S. Murugan, A. Jegan, M. Pannipara, A. G. Al-Sehemi, S. Phang, G. Gnana Kumar and J. Annaraj, *Sens. Actuator B: Chem.*, **2020**, 316, 128082.
12. M. Peng, H. Wang, G. L. Gibson, H. Shang, J. Yang, Y. Chen and Y. Lu, *J. Braz. Chem. Soc.*, **2020**, 31, 305–312.

Supporting information

13. M. Yang, L. Ma, J. Li and L. Kang, *RSC Adv.*, **2019**, *9*, 16812–16818.
14. D. Maheshwaran, T. Nagendraraj, P. Manimaran, B. Ashokkumar, M. Kumar and R. Mayilmurugan, *Eur. J. Inorg. Chem.*, **2017**, 1007–1016.
15. A. Shabbir, S. A. Shahzad, A. Y. A. Alzahrani, Z. A. Khan, M. Yar and W. Rauf, *Spectrochim. Acta Part A: Mol. Biomol. Spectrosc.*, **2025**, *327*, 125414.
16. S. Pang, Y. Yu, W. Wu, J. You, Y. Liang, C. Wu and B. Li, *Luminescence*, **2025**, *40*, e70173.
17. Y. Wang, Y. Chen, Z. Xing and J. Ma, *J. Mol. Struct.*, **2025**, *1313*, 139235.
18. A. Mondal and V. Manivannan, *Spectrochim. Acta Part A: Mol. Biomol. Spectrosc.*, **2024**, *322*, 124734.